4-1-2023

Wideband, High-Gain, and Compact Four-Port MIMO Antenna for Future 5G Devices Operating over Ka-Band Spectrum

Sayed Aqib Hussain
Bahria University

Fatma Taher
Zayed University

Mohammed S. Alzaidi
Taif University

Irshad Hussain
University of Sargodha

Rania M. Ghoniem
Princess Nourah Bint Abdulrahman University

See next page for additional authors

applied sciences

MDPI

Article

Wideband, High-Gain, and Compact Four-Port MIMO Antenna for Future 5G Devices Operating over Ka-Band Spectrum

Sayed Aqib Hussain [1], Fatma Taher [2], Mohammed S. Alzaidi [3], Irshad Hussain [4], Rania M. Ghoniem [5,*], Mohamed Fathy Abo Sree [6] and Ali Lalbakhsh [7,8,*]

1 Department of Electrical Engineering, Bahria University, Islamabad 44000, Pakistan
2 College of Technological Innovation, Zayed University, Dubai 19282, United Arab Emirates
3 Department of Electrical Engineering, College of Engineering, Taif University, P.O. Box 11099, Taif 21944, Saudi Arabia
4 Department of CS and IT, University of Sargodha, Sargodha 40100, Pakistan
5 Department of Information Technology, College of Computer and Information Sciences, Princess Nourah bint Abdulrahman University, P.O. Box 84428, Riyadh 11671, Saudi Arabia
6 Department of Electronics and Communications Engineering, Arab Academy for Science, Technology and Maritime Transport, Cairo 11799, Egypt
7 School of Engineering, Macquarie University, Sydney, NSW 2109, Australia
8 School of Electrical and Data Engineering, University of Technology Sydney, Ultimo, NSW 2007, Australia
* Correspondence: rmghoniem@pnu.edu.sa (R.M.G.); ali.lalbakhsh@mq.edu.au (A.L.)

Abstract: In this article, the compact, ultra-wideband and high-gain MIMO antenna is presented for future 5G devices operating over 28 GHz and 38 GHz. The presented antenna is designed over substrate material Roger RT/Duroid 6002 with a thickness of 1.52 mm. The suggested design has dimensions of 15 mm × 10 mm and consists of stubs with loaded rectangular patch. The various stubs are loaded to antenna to improve impedance bandwidth and obtain ultra-wideband. The resultant antenna operates over a broadband of 26.5–43.7 GHz, with a peak value of gain >8 dBi. A four-port MIMO configuration is achieved to present the proposed antenna for future high data rate devices. The MIMO antenna offers isolation <−30 dB with ECC of <0.0001. The antenna offers good results in terms of gain, radiation efficiency, envelop correlation coefficient (ECC), mean effective gain (MEG), diversity gain (DG), channel capacity loss (CCL), and isolation. The antenna hardware prototype is fabricated to validate the performance of the suggested design of the antenna achieved from software tools, and good correlation between measured and simulated results is observed. Moreover, the proposed work performance is also differentiated with literature work, which verifies that the suggested work is a potential applicant for future 5G compact devices operating over wideband and high gain.

Keywords: wideband antenna; compact size; high gain; Ka-band; 5G

Citation: Hussain, S.A.; Taher, F.; Alzaidi, M.S.; Hussain, I.; Ghoniem, R.M.; Sree, M.F.A.; Lalbakhsh, A. Wideband, High-Gain, and Compact Four-Port MIMO Antenna for Future 5G Devices Operating over Ka-Band Spectrum. *Appl. Sci.* **2023**, *13*, 4380. https://doi.org/10.3390/app13074380

Academic Editor: Naser Ojaroudi Parchin

Received: 3 March 2023
Revised: 24 March 2023
Accepted: 27 March 2023
Published: 30 March 2023

1. Introduction

Due to high data rate and high link capacity, the multiple input and multiple output (MIMO) antenna is widely used in modern wireless communication systems, especially operating over millimeter wave spectrum for 5G devices [1,2]. It also has advantages to avoid seamless connectivity, as in the MIMO system, multiple antennas are installed at transmitter and receiver end. Due to these benefits, a MIMO antenna is a hot trend topic in current research on designing antenna for 5G and 6G communication devices [3,4]. The requirement of the MIMO antenna altered the requirement of antenna designing, as moving towards the MIMO system, the simplified geometry along with low–profile and compact size will be most beneficial [5,6].

On other hand, the performance parameters are also important to examine and analyze, as high data rate and low latency is demanded to facilitate a large number of users with

good services. These demands need an antenna to operate over wideband and offer high gain along with radiation efficiency [7,8]. In the case of the MIMO antenna system, the MIMO parameters are also important to be considered. The mutual coupling, envelop correlation coefficient (ECC), and diversity gain (DG) and many others are key parameters, which will be analyzed [9,10].

In literature, the researcher has present a number of monopole antennas operating over 28 GHz [11–20], and various MIMO systems operational over 28 GHz for wireless communication systems [21–32]. The author of the selected literature reported in [11–14] presents the antenna with compact size and simplified geometry. The setback of these designs is that the report work has a lack of measured results or low gain or radiation efficiency. The antenna reported in [15–19], offers high gain and has simplified geometry. The demerit of these works is narrow operational bandwidth or large size. The requirement of 5G devices is the antenna having a compact size, low profile, and simplified geometry along with wideband and high gain.

According to the requirements of the 5G communication system, the MIMO antenna, which offers a high number of gains, is reported in literature. In [19], the MIMO antenna with improved isolation is proposed by inserting electromagnetic band gap (EBG) between MIMO elements. The reported four-port MIMO antenna operates at 28/38 GHz with a bandwidth of 4 GHz and 2 GHz. Although the antenna is operational over high gain and broadband, it has complex geometry due to inserting EBG cells. A two-port MIMO antenna with simple geometry is reported in [21]. The geometry consists of defected ground structure (DGS) to improve the performance. This work has the demerit of a narrow bandwidth of 1.1 GHz. Another work that offers high gain and wideband is reported in [22]. The antenna consists of eight ports, which lead the reported work with large dimensions.

Compact and wideband antenna operating on mm wave application is reported in [23]. The antenna has a compact size of 24 mm × 20 mm × 1.85 mm and operates over a wideband of 33–44 GHz, but a setback of low value of ECC (that is 0.1). A wideband and high-gain antenna with a bandwidth of 22–50 and peak gain of 15 dBi is reported in [24]. The antenna has complex geometry, as array is adopted to achieve the high gain. In [25], an antenna is presented for the 5G communication system, which offers a bandwidth of 27.1–28.1. The antenna also has large dimensions of 110 mm × 55 mm × 1.6 mm. A compact antenna with an overall size of 12.5 mm × 12.5 mm × 0.8 mm and peak gain of 6 dBi is reported in [26]. The antenna consists of small size and is operational over high gain, but offers low value of other MIMO performance parameters.

A two-port MIMO antenna with geometrical dimensions of 60 mm × 100 mm × 0.965 mm and operating over a bandwidth of 27.6–28.3 GHz and ECC of 0.134. This work has the advantage of simplified geometry, but the demerit of large dimensions, narrow bandwidth, and low value of ECC [27]. A compact MIMO antenna with dimensions of 18.5 mm × 18.5 mm is reported in [28]. The antenna is compact in size and offers a wideband of 4 GHz, but complex geometry due to the multi-layer structure. Another compact antenna with an overall size of 48 mm × 31 mm × 0.254 mm is reported in [29]. The antenna has the advantage of compact size and offers a wideband of 26–31 GHz, but the demerit of high isolation of −21 dB; [30] reports a broad and strong gain. The antenna provides a high gain of 12 dBi and a wideband of 23–40 GHz. This design's setback is substantial, measuring 80 mm by 80 mm by 1.57 mm. The dimensions of a small, high-gain, broadband antenna that operates throughout the frequency range of 25.5 to 30 GHz and has a peak gain of 8.75 dBi are given in [31]. The antenna is small, wideband, and high-gain; however, the authors failed to mention the importance of ECC, and its shape is complicated.

It can be observed from the above discussion and the rest of the literature that the MIMO antenna configuration of the patch antenna is adopted due to its numerous advantages and applications. The ratch antenna with MIMO configuration has an application in smart mobile phones [32] with a high performance parameter and simple geometry, and also in wearable applications when the radiator is placed over flexible substrate

material [33]. To obtain the good results and requirements for 5G applications, various techniques are adopted to improve the performance of the MIMO antenna [34,35]. The most important parameter is mutual coupling between MIMO elements, and some design meta-material is inspired to improve the mutual coupling [36]. The decoupling structure, also called parasitic patch, is loaded between antenna elements to improve isolation [37]. The corner-fed technique [38] and multi-feeding method [39] are also used to get the desired results operational over the 5G spectrum. Moreover, a low-cost MIMO antenna configuration operating over wideband is also adopted for IoT applications [40]. In addition to the patch antenna, Yagi antenna with MIMO configuration is also adopted in the literature for 5G applications [41].

From the above literature review, it is clear that there is still a research gap to design an antenna with compact size, a low profile, and simplified geometry. The antenna should operate over a wideband and offer high gain and radiation efficiency. In this article, the antenna is presented to overcome the demands of a 5G wireless communication system. The antenna offers ultra-wideband and high peak gain. The MIMO parameters also lie according to requirements of any MIMO system. In the rest of the paper, the single element design of the antenna is studied along with results in the form of a S-parameter, gain verses frequency plot, radiation pattern, and radiation efficiency. Afterwards, the MIMO configuration is analyzed, and comparison is performed between measured and simulated results. Last, the comparison table is added to compare the results of proposed antenna with literature along with conclusion and references.

The novelty of proposed work is:

- The compact size and simplified geometry;
- Wide operational band and high gain;
- Low mutual coupling between MIMO elements;
- Good values of MIMO parameters, such as, ECC, CCL, DG, and MEG.

2. Wideband Antenna Designing

2.1. Design Methodology

Figure 1 depicts the structure of the suggested design of an antenna operating over 28 GHz. The antenna is designed over substrate material Roger RT/Duroid 6002 with a loss tangent of 0.0012 and relative permittivity of 2.2. The antenna has an overall size of L $\times$ W $\times$ H = 15 mm $\times$ 10 mm $\times$ 1.52 mm. The antenna has a simplified structure with a rectangular and circular patch loaded with arm-shaped stubs. These stubs are loaded to the antenna to improve antenna performance in terms of bandwidth and return loss. Moreover, the antenna is designed on the commercially available electromagnetic (EM) software tool high frequency structure simulator (HFSSv9). The optimized value of antenna parameters is given below. W = 10; L = 15; H = 1.52; A = 2; B = 2.58; C = 4; D = 4; E = 1; F_X = 6; F_Y = 0.75; and R = 2. All units are in millimeters (mm).

To obtain the optimized results, few design steps are performed. Initially, an antenna with rectangular stub is design in first step for 28/38 GHz wireless applications. The length and width of the antenna are obtained from the below formula [42,43]:

$$L_{eff} = \frac{c}{2F\sqrt{\varepsilon reff}} \tag{1}$$

$$\varepsilon_{reff} = \frac{\varepsilon r + 1}{2} + \frac{\varepsilon r - 1}{2}\left[\frac{1}{1 + 12\,\frac{H}{W}}\right] \tag{2}$$

$$\Delta L = 0.412H\,\frac{(\varepsilon reff + 0.3)\left(\frac{W}{H} + 0.264\right)}{(\varepsilon reff - 0.258)\left(\frac{W}{H} + 0.8\right)} \tag{3}$$

The resultant antenna operates at 28 GHz and 37 GHz with a return loss of -10.25 dB and -8.5 dB, respectively. After that, in the second step, a circular radiator of radius

R = 2 mm is loaded to the antenna in order to improve the return loss, which will help in the enhancement of bandwidth. The antenna obtained from this step offers multiple resonances at 25 GHz, 29 GHz, 38 GHz, and 42 GHz with return losses of −12.5 dB, −15 dB, −16 dB, and −14.35 dB, respectively. In the third stage, an arm-shaped stub is added as given in the figure. This step improves the return loss of the antenna, which leads the antenna to operate over a wideband. In the final stage, the length of the arm is improved to get further improvement in the bandwidth of the antenna. The improvement is possible until the length of 4 mm. The antenna obtained from the final stage offers ultra-wideband from 26.5 to 43.7 GHz, as given in Figure 2.

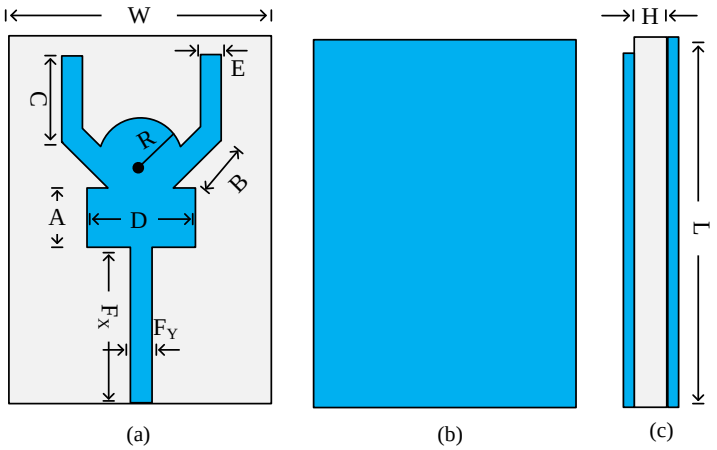

Figure 1. Geometrical configuration of proposed a dual-band millimeter wave antenna: (**a**) top view, (**b**) back view, and (**c**) side view.

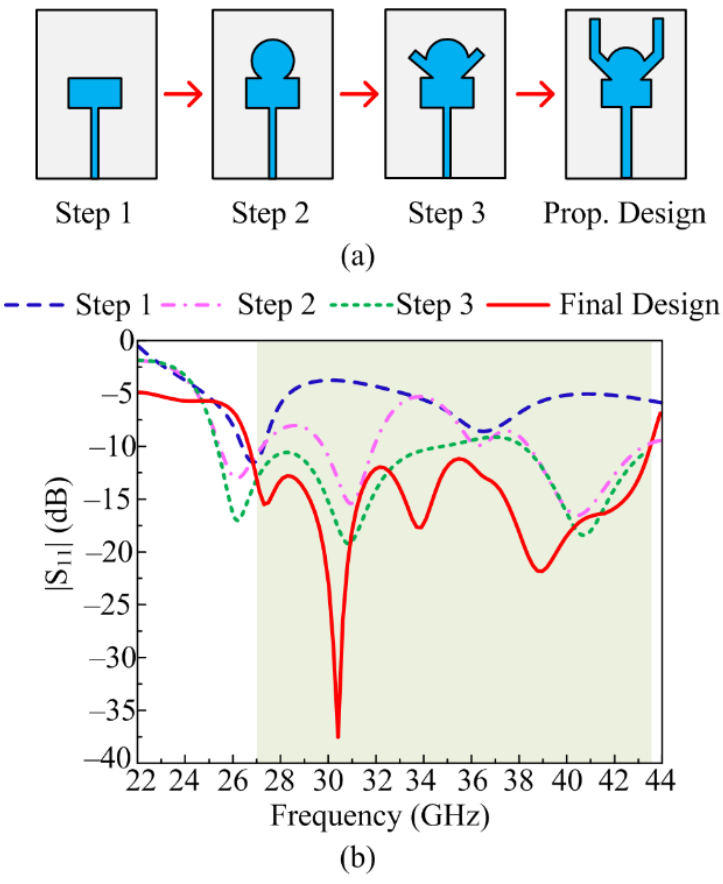

Figure 2. (**a**) Designing steps; (**b**) corresponding results.

Parametric analysis of key parameters is performed to get an optimized value. For the proposed antenna, the parametric analysis radius of the circular patch and length of the lower stub is analyzed. At an optimal value of R = 1.8 mm, the antenna offers the ultra-wideband of 26.5–43.7 GHz with a minimum value of return loss around −38 dB. If the value is increased to 2.0 mm, the antenna stops operating over wideband and only offers dual band with a minimum return loss of −18 dB and −11 dB at a resonant frequency of 29.5 GHz and 38.5 GHz, respectively. If the value is decreased to 1.6 mm, again the return loss and bandwidth is compromised, as given in Figure 3a. Another key parameter is the length of lower stub D. At optimal value of D = 4 mm, the antenna offers the required operational band. If the value is fixed at D = 6 mm, the antenna offers a 30–37 GHz bandwidth with a return loss of around −15 dB. If the value is fixed at D = 2 mm, the antenna offers 31.5–42.5 GHz with a return loss of around −20 dB, as given in Figure 3b.

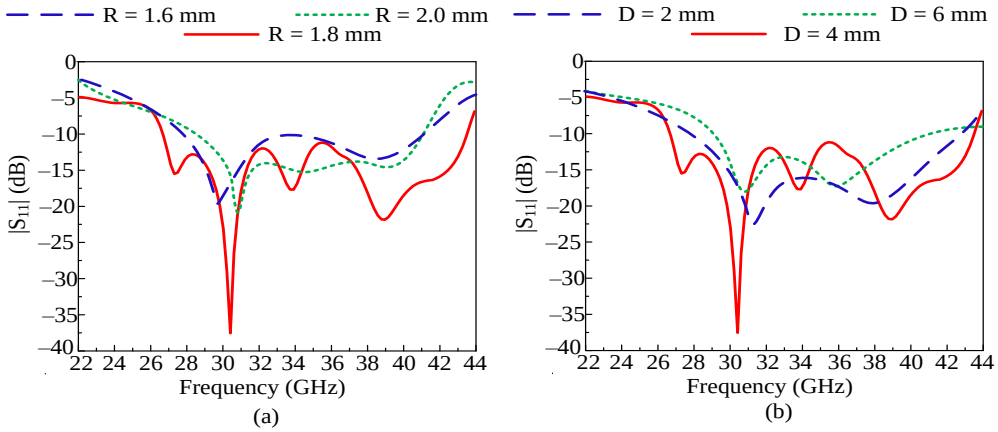

Figure 3. Parametric analysis of (**a**) the radius of the circular patch and (**b**) length of the lower stub.

2.2. Results of Unit Elements

To validate the performance of the antenna, the important parameters are analyzed. For further clarification, the hardware prototype is fabricated to compare with simulated results, as shown in Figure 4. In this section, various performance parameters are discussed and compared with measured results.

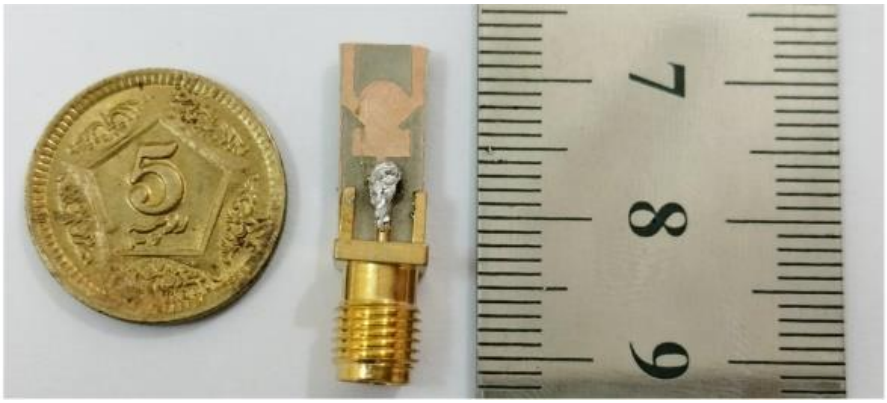

Figure 4. Fabricated prototype of wideband antenna.

2.2.1. $|S_{11}|$

Figure 5 represents the comparison between the measured and simulated S-parameter of the proposed ultra-wideband antenna. It can be seen from the figures that the antenna offers broadband ranging from 26.5 to 43.7 GHz with resonance frequencies of 30 GHz, 34, and 38 GHz. The proposed work covers the 5G band for millimeter wave application. The antenna offers a low value of return loss with a minimum −38 dB and maximum −15 dB.

The results also show similarity between simulated and measured results, which makes the proposed work the best applicant for future 5G devices operating at broadband.

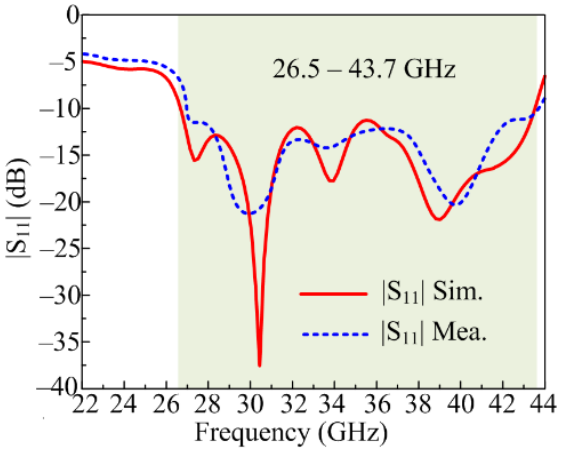

Figure 5. Comparison among simulated and experimental $|S_{11}|$ results.

2.2.2. Gain

Figure 6 shows a comparison of the proposed antenna's prototype gain and software-predicted gain. At the resonance frequency of 30 GHz, the antenna delivers a peak gain of >8 dB. It may be noted from the figures that the antenna delivers gain >6.5 dBi at an operational bandwidth of 26.5–43.7 GHz. The suggested antenna is the best candidate for future 5G devices using wideband and high gain because of the great agreement between predicted and tested outcomes.

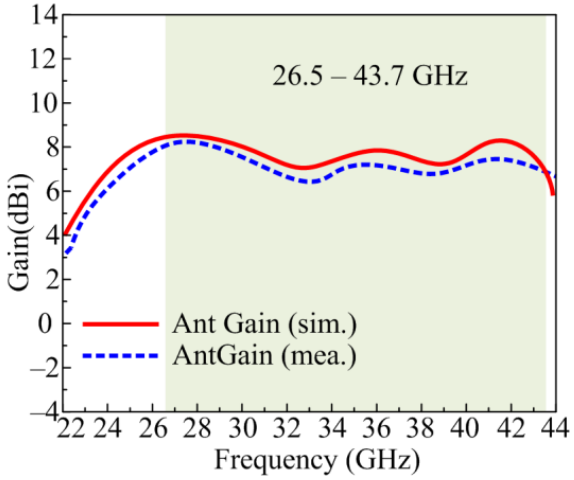

Figure 6. Comparison among simulated and experimental gain results.

2.2.3. Radiation Pattern

The proposed ultra-wideband antenna's observed and modelled radiation patterns at resonance frequencies of 30 GHz and 28 GHz are shown in Figure 7a,b. It is clear that the antenna provides both frequencies with a broad side radiation pattern in the E-plane and a slightly inclined radiation pattern in the H-plane. The tiny distortion in the radiation pattern is due to loading several stubs. Both the generated and observed radiation patterns exhibit strong correlations with one another. When testing, a little discrepancy that results from manufacturing flaws or connection loss is noticed. Because of the results and correlation between measured and simulated outcomes, future 5G devices running at broadband and high gain may be interested in the proposed study. The antenna offers a low cross polarization of <-14 dB for both resonating frequencies.

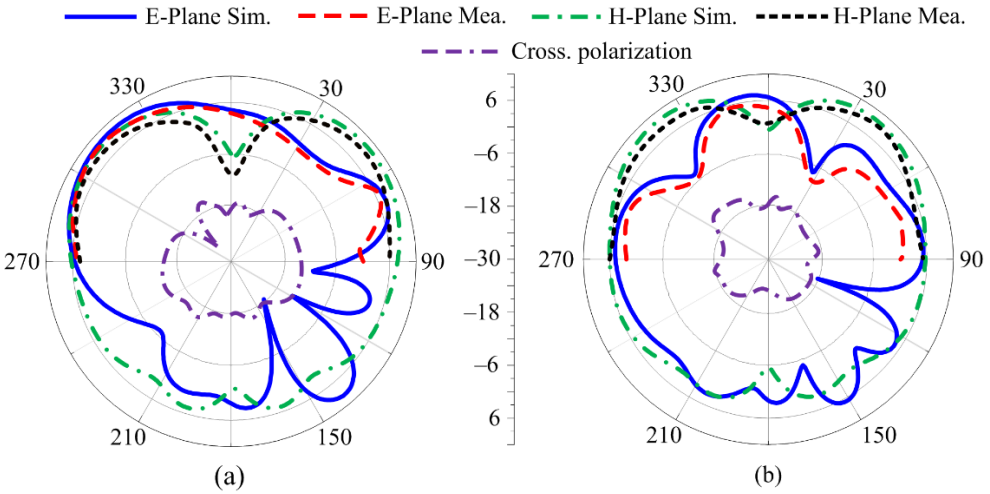

Figure 7. Radiation pattern and cross-polarization of a single element at (**a**) 28 GHz and (**b**) 38 GHz.

2.2.4. Surface Current Density

Figure 8 shows the surface current distribution of the proposed antenna operating over the ultra-wideband of 26.5–43.7 GHz. It can be seen from the figures that the current is highly distributed at feedlines and arm stubs for 28 GHz and the feedline and the lower part of the antenna for 38 GHz. This phenomenon refers to that larger the effective electrical length, which proves the generation of resonances. Moreover, the large number of current distributions at arms also verifies the wideband operation of the antenna by loading these stubs.

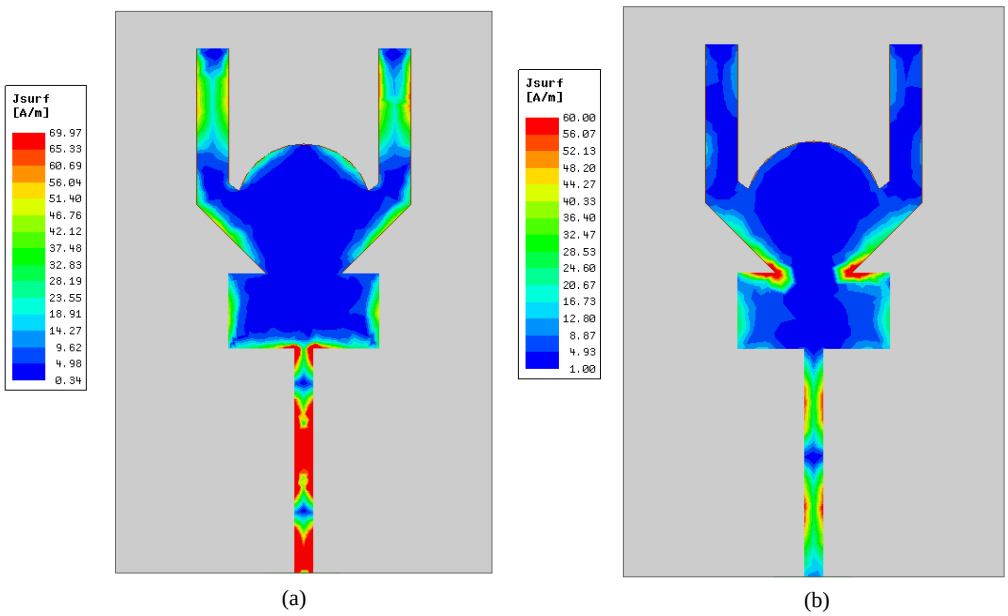

Figure 8. Surface current distribution of the proposed single element of antenna (**a**) 28 GHz and (**b**) 38 GHz.

2.2.5. Radiation Efficiency

Figure 9 shows the proposed antenna's predicted radiation efficiency. The antenna has a strong radiation pattern with a 26.5–42.7 GHz working bandwidth. At resonance frequencies of 30 GHz and 38 GHz, the antenna yields peak values of 86% and 90%, respectively, with peak values of around >82% at operating bandwidth.

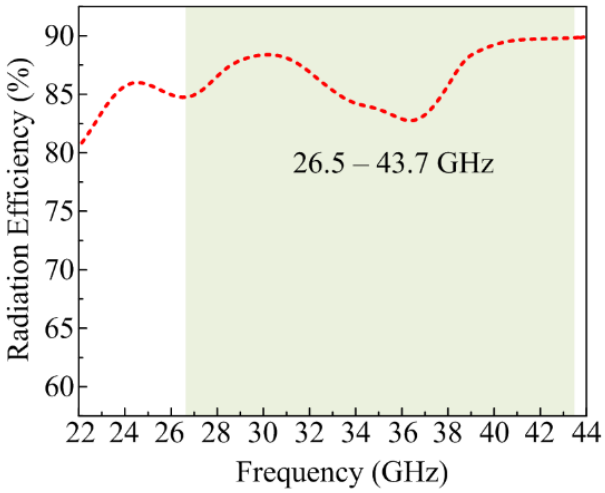

Figure 9. Simulated radiation efficiency of proposed antenna.

3. Four-Port MIMO Antenna

In this section, the MIMO configuration of the proposed antenna along with the hardware prototype is discussed. The antenna results, along with MIMO performance parameter, are also studied.

3.1. MIMO Antenna Design

Figure 10a shows the four-port MIMO antenna for ultra-wideband and high gain applications. The proposed MIMO antenna has an overall size of $M_Y \times M_X \times H = 27$ mm $\times$ 27 mm $\times$ 1.52 mm and is designed over same material as the single element. Each unit element of the MIMO antenna has the same dimension as the single element given in Figure 1. The gap between two adjacent elements M1 = 4 mm and between two opposite elements is $M_2 = 10.2$ mm. Moreover, the hardware prototype is fabricated to verify the simulated results, as depicted in Figure 9b.

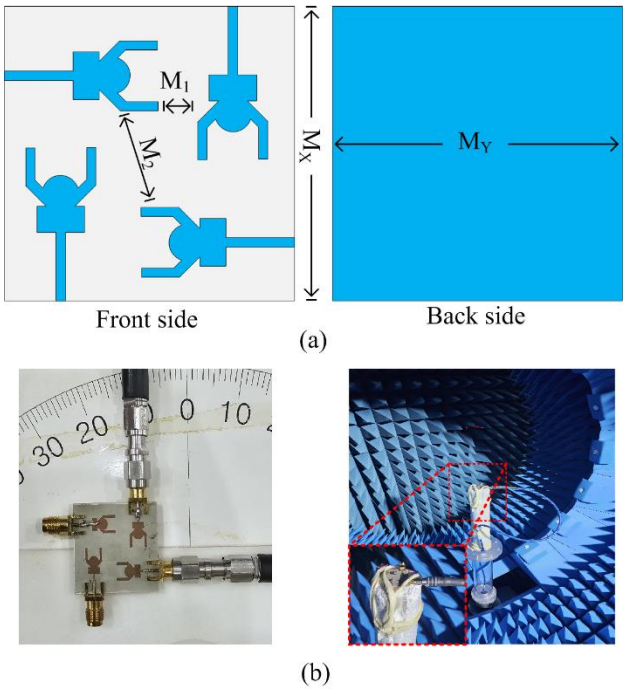

Figure 10. (**a**) Configuration of proposed MIMO antenna; (**b**) measurement setup for S-parameters and far-field parameters.

3.2. Results and Discussion

3.2.1. S-parameters

Figure 11 depicts the simulated and measured reflection and transmission coefficient of the proposed four-port ultra-wideband MIMO antenna. It can be seen that the antenna offers a broadband of 26.5–41.7 GHz with resonance frequencies of 30 GHz, 33 GHz, and 38 GHz. It can also be observed from the figures that each element of the MIMO antenna shows good correlation with each other, as well as with measured results. On other hand, the figure also shows the transmission the coefficient of the proposed antenna. According to the figures, the antenna offers minimum isolation around −55 dB and maximum isolation around −35 dB for nearby element and minimum isolation of −52 dB and maximum isolation of −32 dB with adjacent element. The results in the form of transmission and reflection coefficient and strong agreement between simulated and measured results, making the proposed MIMO antenna a good applicant for future 5G devices operating over broadband applications.

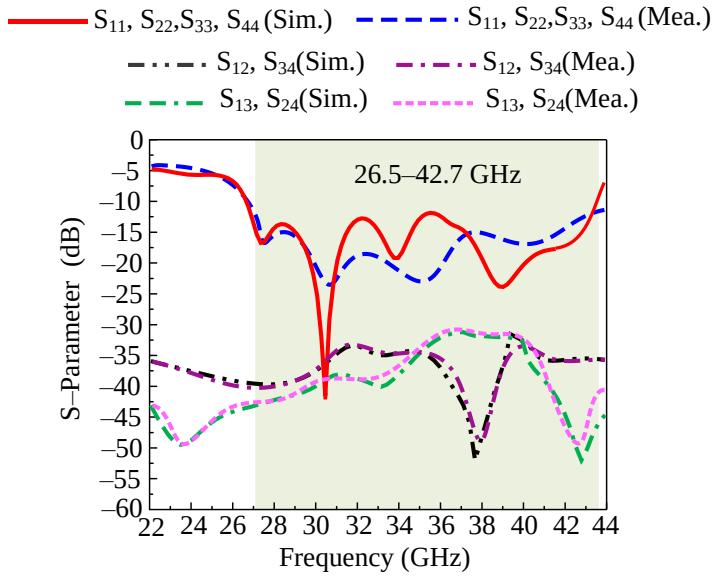

Figure 11. Comparison among S-parameters of MIMO antenna.

The minor difference between measured and simulated results may be due to:

- The fabrication tolerance of apparatus used for fabrication of antenna;
- Measurement setup tolerance due to usage of old wires;
- Connectors used in measurements as mismatching occur due to connectors at higher frequency due to increase in losses on connectors.

3.2.2. Radiation Pattern of MIMO Antenna

Figure 12 shows the ultra-wideband MIMO antenna's observed and predicted radiation pattern at resonance frequencies of 30 GHz and 38 GHz. It is clear that the antenna provides both frequencies with a broad side radiation pattern in the E-plane and a slightly inclined radiation pattern in the H-plane. The loading of several stubs is what caused the little distortion in the radiation pattern. Both the generated and observed radiation patterns exhibit strong correlations with one another. When testing, a little discrepancy that results from manufacturing flaws or connection loss is found. Because of the results and correlation between measured and simulated outcomes, future 5G devices running at broadband and high gain may be interested in the proposed study. Moreover, low cross-polarization of <-10 dB is observed for both frequencies.

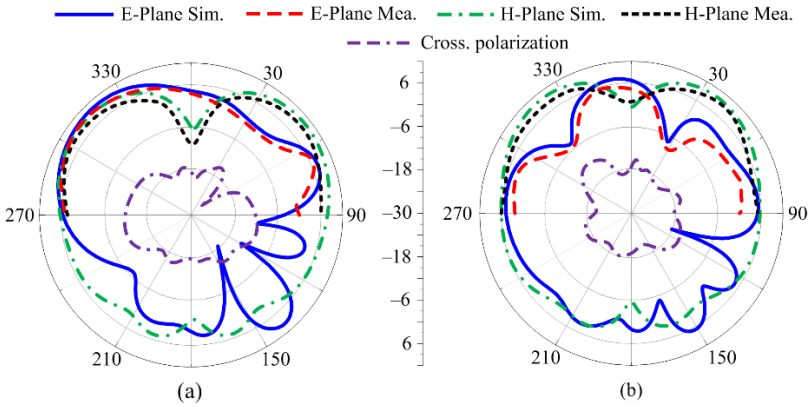

Figure 12. Radiation pattern and cross polarization of proposed MIMO antenna at (**a**) 28 GHz and (**b**) 38 GHz.

3.2.3. Electric Field Distribution

Figure 13 shows the E-field distribution of proposed MIMO antenna operating over an ultra-wideband of 26.5–42.7 GHz. It can be observed that most of the electric field is distributed among the feedline and the bottom rectangular patch for non-operating MIMO elements.

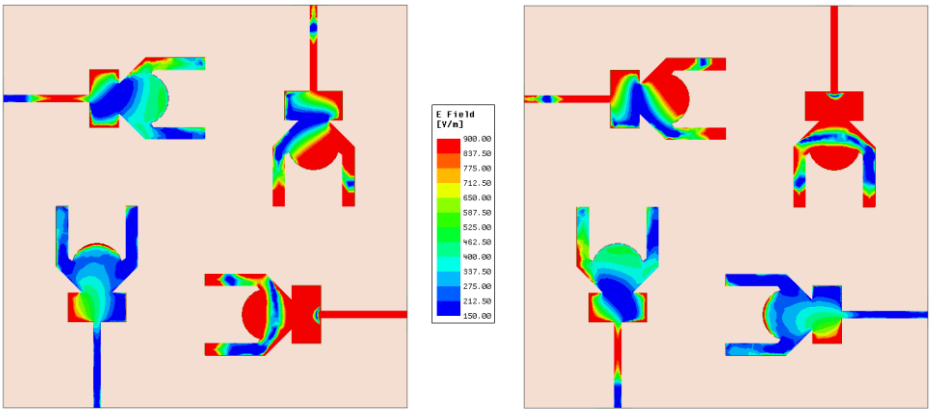

Figure 13. Electric filed distribution of proposed single element of antenna (**a**) 28 GHz and (**b**) 38 GHz.

3.2.4. Envelop Correlation Coefficient

By examining the envelope correlation coefficient (ECC), it is possible to evaluate the performance of a single MIMO antenna element. It may be measured using the S-parameter and the pattern of distant radiation. The ECCs of the adjustment element and diagonal element for the proposed ultra-wideband MIMO antenna are shown in Figure 14. As can be observed, the antenna operates over a wideband of 26.5–42.7 GHz with an ECC of 0.001. The following mathematical formulas (4) may be used to compute the ECC of a MIMO antenna [44]:

$$|\rho_e(i,j,N)| = \frac{\left|\sum_{n=1}^{N} S_{i,n}S_{n,j}\right|}{\sqrt{\left|\prod_{k(=i,j)}\left[1-\sum_{n-1}^{N} S_{i,n}S_{n,k}\right]\right|}} \quad (4)$$

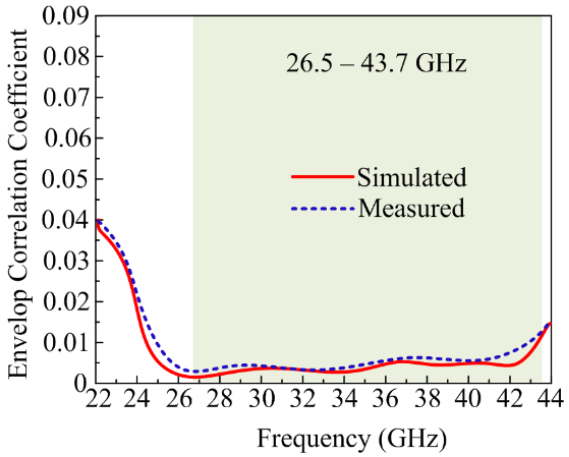

Figure 14. ECC of the proposed MIMO antenna.

In the above equation, i and j are antenna elements and N represents number of antennas placed in MIMO systems.

3.2.5. Diversity Gain

By using a MIMO antenna system, there are transmission power losses that may be examined by looking at diversity gain (DG). In the best-case situation, the value DG = 10 dB; however, in real-world scenarios, a value near 10 dB is taken into account. According to Figure 15, the suggested ultra-wideband MIMO antenna provides DG of about 9.99 dB over an operational bandwidth of 26.5–42.7 GHz. Equation (5) provided in [45,46] may be used to quantitatively compute the DG of a MIMO antenna system.

$$DG = 10\sqrt{1-|ECC|^2} \quad (5)$$

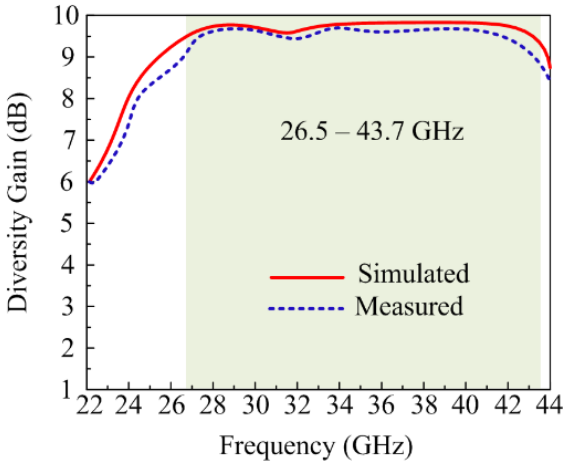

Figure 15. Comparison among predicted and measured DG.

3.2.6. Channel Capacity Loss

Channel capacity losses also happen as a result of correlation losses in MIMO antennas. It is a crucial component of every MIMO antenna. The value of CCL is observed for the proposed ultra-wideband MIMO antenna at about 0.01 bps/Hz over the operational bandwidth of 26.5–42.7 GHz, as shown in Figure 16. The value of CCL in an ideal situation is in the vicinity of 0.5 bps/Hz. The Formula (6) to compute CCL is shown below [45,46].

$$C_{Loss} = -log_2 \det\left(\propto^R\right) \quad (6)$$

where

$$\propto^R = \begin{bmatrix} \propto_{11} & \propto_{12} \\ \propto_{21} & \propto_{22} \end{bmatrix}$$

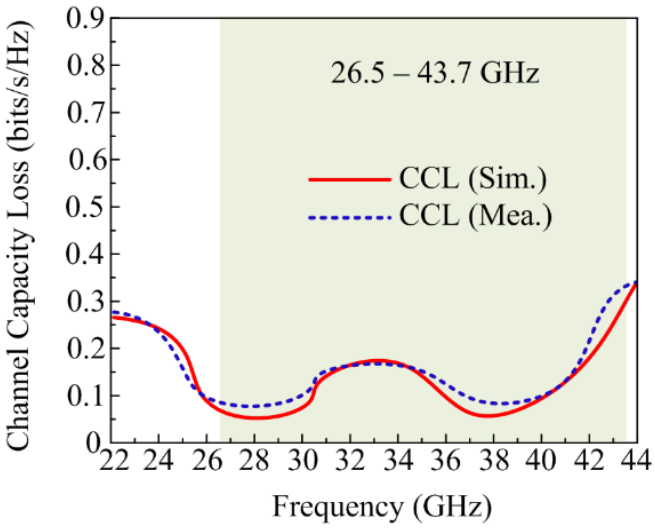

Figure 16. CCL of the proposed work.

3.2.7. Mean Effective Gain

By examining the mean effective gain, the received power of a MIMO antenna system in a fading environment may be examined (MEG). The ideal instance would have an MEG value of less than 3 dBi. According to Figure 17, the suggested ultra-wideband MIMO antenna gives MEG −8 dBi at an operating bandwidth of 26.5–42.7 GHz. Moreover, the following Equation (7), provided in [45,46], may be used to compute the MEG of a MIMO antenna:

$$MEG_i = \frac{P_{rec}}{P_{inc}} = \oint \left[\frac{XPR.\, G_{\theta i}(\Omega) + G_i(\Omega).P(\Omega)}{1 + XPR} \right] d\Omega \quad (7)$$

where $P_{\varnothing}$ represents an angular density function of incident power and XPR is the cross-polarization power ratio.

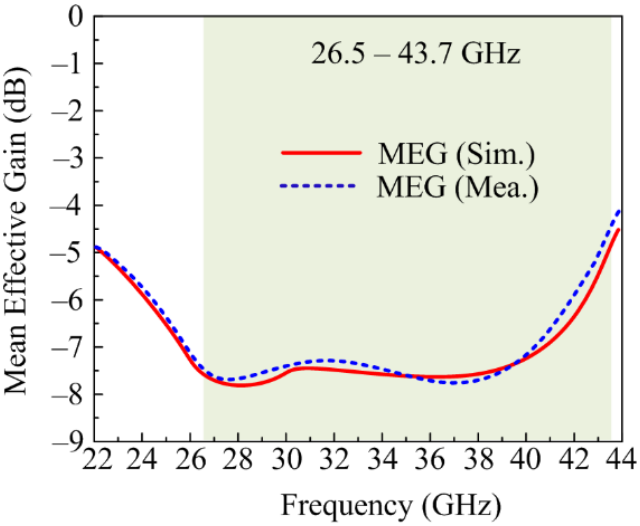

Figure 17. MEG of the proposed MIMO antenna.

3.3. Performance Comparison

Table 1 provides a comparison of the proposed ultra-wideband antenna operating over 26.5–43.7 GHz with the antenna already published in literature. The comparison in terms of size, number of ports, operational bandwidth, peak gain, ECC, and minimum/maximum isolation is performed. It can be seen from the table that antenna has compact size, offers wideband and high gain, along with good and acceptable values of ECC and isolation. This comparison also makes the proposed antenna a good applicant for future 5G devices having a compact size and operating over wideband and high gain.

Table 1. Comparison between suggested and literature works operating over same frequency.

Ref	Dimensions (mm × mm × mm)	Ports	Bandwidth (GHz)	Operating Frequency (GHz)	Peak Gain (dBi)	ECC	Mini. Isolation (dB)	Max. Isolation (dB)	MIMO Antenna Type
[18]	115 × 60 × 0.76	5	27.5–28.7	28.3	5	0.056	−30	−13	Monopole antenna
[19]	50.8 × 12.5 × 0.8	4	26–36	27	5.23	–	−45	−22	CPW-fed patch antenna
[20]	19.25 × 26 × 0.79	4	27–30.5	28.5	7.58	0.001	−35	−12	EBG-based antenna
[23]	24 × 20 × 1.85	4	33–44.1	38	4.56	0.1	−32	−16	Patch antenna over transparent substrate
[24]	53 × 20 × 0.203	2	22–50	36/45	15	0.12	−40	−20	Slot array antenna
[25]	110 × 55 × 1.6	6	27.7–28.7	28	5.13	0.005	−55	−22	Air-filled slotted loop (AFSL) antenna
[26]	12.5 × 12.5 × 0.8	4	33–36	35	6	0.02	−33	−23	Hexagonal patch antenna
[27]	60 × 100 × 0.965	2	27.6–28.3	28	4.5	0.134	−30	−17	Modified monopole antenna
[29]	48 × 31 × 0.254	4	26–31	28	10	0.0015	−38	−21	Patch antenna loaded with array of meatmaterials
[30]	80 × 80 × 1.57	4	23–40	30	12	0.0014	−40	−20	Arc-shaped patch antenna
[31]	20.5 × 12 × 0.79	2	25.5–30	28	8.75	–	−40	−30	E-shaped patch antenna
Prop. Work	27 × 27 × 1.52	4	26.5–43.7	30/38	8.4	0.001	−42	−30	Stub loaded monopole antenna

4. Conclusions

This article presents the design and validation of a wideband antenna for Ka-band 5G applications. The initial design is comprised of a rectangular printed antenna, whose performance is enhanced using an additional circular patch along with the loading of two open-ended stubs. The resultant antenna offers wideband ranges from 26.5 GHz to 43.7 GHz having a peak gain of >6 dBi in the operational band. The unit element had a compact size of 10×15 mm^2. Furthermore, to meet the requirements of the modern-day devices, a MIMO antenna is constructed using elements. The consecutive elements are placed orthogonal to achieve a low mutual coupling. Moreover, the presence of the open-ended stubs further helps to lower mutual coupling. The edge-to-edge space between consecutive elements is 4 mm and the maximum mutual coupling is less than −30 dB. Other performance parameters of the MIMO antenna are also studied, which show acceptable values in all terms. At last, the performance comparison is performed with recently reported works and the proposed work overperforms all the works by offering wideband, compact size, high gain, and low mutual coupling, making the proposed work a potential candidate for ka-band applications. The future extension of the proposed work is to deploy it for massive MIMO applications requiring the low mutual coupling among the element placed in close range.

Author Contributions: Conceptualization, methodology, software, validation, S.A.H., F.T., M.S.A. and I.H.; formal analysis, investigation, resources, data curation, R.M.G., M.F.A.S. and A.L.; writing—original draft preparation, S.A.H., I.H. and F.T.; writing—review and editing, M.S.A., R.M.G., M.F.A.S. and A.L.; visualization, R.M.G.; supervision, A.L.; project administration, funding acquisition, R.M.G. and A.L. All authors have read and agreed to the published version of the manuscript.

Funding: Princess Nourah bint Abdulrahman University Researchers Supporting Project number (PNURSP2023R138), Princess Nourah bint Abdulrahman University, Riyadh, Saudi Arabia.

Institutional Review Board Statement: Not applicable.

Informed Consent Statement: Not applicable.

Data Availability Statement: All data is included in the study.

Acknowledgments: We acknowledge the support from Princess Nourah bint Abdulrahman University Researchers Supporting Project number (PNURSP2023R138), Princess Nourah bint Abdulrahman University, Riyadh, Saudi Arabia.

Conflicts of Interest: The authors declare no conflict of interest.

References

1. Rappaport, T.S.; Sun, S.; Mayzus, R.; Zhao, H.; Azar, Y.; Wang, K.; Wong, G.N.; Schulz, J.K.; Samimi, M.; Gutierrez, F. Millimeter wave mobile communications for 5G cellular: It will work! *IEEE Access* **2013**, *1*, 335–349. [CrossRef]
2. Hussain, M.; Awan, W.A.; Alzaidi, M.S.; Hussain, N.; Ali, E.M.; Falcone, F. Metamaterials and their application in the performance enhancement of reconfigurable antennas: A review. *Micromachines* **2023**, *14*, 349. [CrossRef] [PubMed]
3. Kulkarni, J.; Sim, C.Y.D.; Gangwar, R.K.; Anguera, J. Broadband and compact circularly polarized MIMO antenna with concentric rings and oval slots for 5G application. *IEEE Access* **2022**, *10*, 29925–29936. [CrossRef]
4. Rosaline, I.; Kumar, A.; Upadhyay, P.; Murshed, A.H. Four element MIMO antenna systems with decoupling lines for high-speed 5G wireless data communication. *Int. J. Antennas Propag.* **2022**, *2022*, e9078929. [CrossRef]
5. Hei, Y.Q.; He, J.G.; Li, W.T. Wideband Decoupled 8-Element MIMO Antenna for 5G Mobile Terminal Applications. *IEEE Antennas Wirel. Propag. Lett.* **2021**, *20*, 1448–1452. [CrossRef]
6. Hussain, M.; Awan, W.A.; Ali, E.M.; Alzaidi, M.S.; Alsharef, M.; Elkamchouchi, D.H.; Alzahrani, A.; Fathy Abo Sree, M. Isolation improvement of parasitic element-loaded dual-band MIMO antenna for mm-Wave applications. *Micromachines* **2022**, *13*, 1918. [CrossRef]
7. Ali, E.M.; Awan, W.A.; Naqvi, S.I.; Alzaidi, M.S.; Alzahrani, A.; Elkamchouchi, D.H.; Falcone, F.; Alharbi, T.E.A. A low-profile antenna for on-body and off-body applications in the lower and upper ISM and WLAN bands. *Sensors* **2023**, *23*, 709. [CrossRef]
8. Tang, H.; Bulger, C.J.; Rovere, T.; Zheng, B.; An, S.; Li, H.; Dong, Y.; Haerinia, M.; Fowler, C.; Gonya, S.; et al. A Low-Profile Flexible Dual-Band Antenna with Quasi-Isotropic Radiation Patterns for MIMO System on UAVs. *IEEE Antennas Wirel. Propag. Lett.* **2022**, *22*, 49–53. [CrossRef]
9. Affandi, A.; Azim, R.; Alam, M.M.; Islam, M.T. A low-profile wideband antenna for WWAN/LTE applications. *Electronics* **2020**, *9*, 393. [CrossRef]
10. Zaidi, A.; Awan, W.A.; Ghaffar, A.; Alzaidi, M.S.; Alsharef, M.; Elkamchouchi, D.H.; Ghoneim, S.S.M.; Alharbi, T.E.A. A low profile ultra-wideband antenna with reconfigurable notch band characteristics for smart electronic systems. *Micromachines* **2022**, *13*, 1803. [CrossRef]
11. Hussain, M.; Ali, E.M.; Awan, W.A.; Hussain, N.; Alibakhshikenari, M.; Virdee, B.S.; Falcone, F. Electronically reconfigurable and conformal triband antenna for wireless communications systems and portable devices. *PLoS ONE* **2022**, *17*, e0276922. [CrossRef] [PubMed]
12. Hussain, M.; Hussain, A.; Alibakhshikenari, M.; Falcone, F.; Limiti, E. A simple geometrical frequency reconfigurable Antenna with Miniaturized Dimensions for 24.8/28GHz 5G Applications. In Proceedings of the 2022 16th European Conference on Antennas and Propagation (EuCAP), Madrid, Spain, 27 March–1 April 2022; pp. 1–3.
13. Kamal, M.M.; Yang, S.; Kiani, S.H.; Sehrai, D.A.; Alibakhshikenari, M.; Abdullah, M.; Falcone, F.; Limiti, E.; Munir, M. A novel hook-shaped antenna operating at 28 GHz for future 5G mmwave applications. *Electronics* **2021**, *10*, 673. [CrossRef]
14. Zahra, H.; Awan, W.A.; Ali, W.A.E.; Hussain, N.; Abbas, S.M.; Mukhopadhyay, S. A 28 GHz Broadband Helical Inspired End-Fire Antenna and Its MIMO Configuration for 5G Pattern Diversity Applications. *Electronics* **2021**, *10*, 405. [CrossRef]
15. Ibrahim, A.A.; Zahra, H.; Dardeer, O.M.; Hussain, N.; Abbas, S.M.; Abdelghany, M.A. Slotted Antenna Array with Enhanced Radiation Characteristics for 5G 28 GHz Communications. *Electronics* **2022**, *11*, 2664. [CrossRef]
16. Ullah, H.; Abutarboush, H.F.; Rashid, A.; Tahir, F.A. A Compact Low-Profile Antenna for Millimeter-Wave 5G Mobile Phones. *Electronics* **2022**, *11*, 3256. [CrossRef]
17. Kumar, P.; Ali, T.; Kumar, O.P.; Vincent, S.; Kumar, P.; Nanjappa, Y.; Pathan, S. An Ultra-Compact 28 GHz Arc-Shaped Millimeter-Wave Antenna for 5G Application. *Micromachines* **2023**, *14*, 5. [CrossRef]
18. Ikram, M.; Sharawi, M.S.; Shamim, A. A novel very wideband integrated antenna system for 4G and 5G mm-wave applications. *Microw. Opt. Technol. Lett.* **2017**, *59*, 3082–3088. [CrossRef]
19. Jilani, S.F.; Abbasi, Q.H.; Imran, M.A.; Alomainy, A. Design and Analysis of Millimeter-Wave Antennas for the Fifth Generation Networks and Beyond. In *Wiley 5G Ref: The Essential 5G Reference Online*; Wiley Online Library: New York, NY, USA, 2019; pp. 1–21.
20. Tu, D.T.T.; Thang, N.G.; Ngoc, N.T.; Phuong, N.T.B.; Van Yem, V. 28/38 GHz dual-band MIMO antenna with low mutual coupling using novel round patch EBG cell for 5G applications. In Proceedings of the International Conference on Advanced Technologies for Communications (ATC), Quy Nhon, Vietnam, 18–20 October 2017; pp. 64–69.

21. Xing, H.; Wang, X.; Gao, Z.; An, X.; Zheng, H.-x.; Wang, M.; Li, E. Efficient Isolation of an MIMO Antenna Using Defected Ground Structure. *Electronics* **2020**, *9*, 1265. [CrossRef]
22. Abdullah, M.; Kiani, S.H.; Iqbal, A. Eight element multiple-input multiple-output (MIMO) antenna for 5G mobile applications. *IEEE Access* **2019**, *7*, 134488–134495. [CrossRef]
23. Desai, A.; Bui, C.D.; Patel, J.; Upadhyaya, T.; Byun, G.; Nguyen, T.K. Compact wideband four element optically transparent MIMO antenna for mm-wave 5G applications. *IEEE Access* **2020**, *8*, 194206–194217. [CrossRef]
24. Saad, A.A.R.; Mohamed, H.A. Printed millimeter-wave MIMO-based slot antenna arrays for 5G networks. *AEU Int. J. Electron. Commun.* **2019**, *99*, 59–69. [CrossRef]
25. Marzouk, H.M.; Ahmed, M.I.; Shaalan, A.A. *A Novel Dual-Band 28/38 GHz AFSL MIMO Antenna for 5G Smartphone Applications*; Journal of Physics: Conference Series; IOP Publishing: Bristol, UK, 2020; Volume 1447.
26. Elfergani, I.; Rodriguez, J.; Iqbal, A.; Sajedin, M.; Zebiri, C.; AbdAlhameed, R.A. Compact millimeter-wave MIMO antenna for 5G applications. In Proceedings of the 14th European Conference on Antennas and Propagation (EuCAP), Copenhagen, Denmark, 15–20 March 2020; pp. 1–5.
27. Alreshaid, A.T.; Hussain, R.; Podilchak, S.K.; Sharawi, M.S. A dual-element MIMO antenna system with a mm-wave antenna array. In Proceedings of the 2016 10th European conference on antennas and propagation (EuCAP), Davos, Switzerland, 10–15 April 2016; pp. 1–4.
28. Arabi, O.; See, C.H.; Ullah, A.; Ali, N.; Liu, B.; Abd-Alhameed, R.; McEwan, N.J.; Excell, P.S. Compact Wideband MIMO Diversity Antenna for Mobile Applications Using Multi-Layered Structure. *Electronics* **2020**, *9*, 1307. [CrossRef]
29. Wani, Z.; Abegaonkar, M.P.; Koul, S.K. A 28-GHz antenna for 5G MIMO applications. *Prog. Electromagn. Res. Lett.* **2018**, *78*, 73–79. [CrossRef]
30. Sehrai, D.A.; Abdullah, M.; Altaf, A.; Kiani, S.H.; Muhammad, F.; Tufail, M.; Irfan, M.; Glowacz, A.; Rahman, S. A novel high gain wideband MIMO antenna for 5G millimeter wave applications. *Electronics* **2020**, *9*, 1031. [CrossRef]
31. Taher, F.; Hamadi, H.A.; Alzaidi, M.S.; Alhumyani, H.; Elkamchouchi, D.H.; Elkamshoushy, Y.H.; Haweel, M.T.; Sree, M.F.A.; Fatah, S.Y.A. Design and analysis of circular polarized two-port MIMO antennas with various antenna element orientations. *Micromachines* **2023**, *14*, 380. [CrossRef]
32. Dayo, Z.A.; Aamir, M.; Rahman, Z.; Khoso, I.A.; Lodro, M.M.; Dayo, S.A.; Soothar, P.; Pathan, M.S.; Al-Gburi, A.J.A.; Memon, A.A.; et al. A Novel Low-Cost Compact High-Performance Flower-Shaped Radiator Design for Modern Smartphone Applications. *Micromachines* **2023**, *14*, 463. [CrossRef] [PubMed]
33. Saeidi, T.; Al-Gburi, A.J.A.; Karamzadeh, S. A Miniaturized Full-Ground Dual-Band MIMO Spiral Button Wearable Antenna for 5G and Sub-6 GHz Communications. *Sensors* **2023**, *23*, 1997. [CrossRef]
34. Khan, A.; He, Y.; He, Z.; Chen, Z.N. A Compact Quadruple-Band Circular Polarized MIMO Antenna With Low Mutual Coupling. *IEEE Trans. Circuits Syst. II Express Briefs* **2023**, *70*, 501–505. [CrossRef]
35. Liu, J.; Liu, H.; Dou, X.; Tang, Y.; Zhang, C.; Wang, L.; Tang, R.; Yin, Y. A low profile, dual-band, dual-polarized patch antenna with antenna-filter functions and its application in MIMO systems. *IEEE Access* **2021**, *9*, 101164–101171. [CrossRef]
36. Khan, A.; He, Y.; Chen, Z.N. An Eight-Port Circularly Polarized Wideband MIMO Antenna Based on a Metamaterial-Inspired Element for 5G mmWave Applications. *IEEE Antennas Wirel. Propag. Lett.* **2023**. [CrossRef]
37. Ali, W.A.E.; Ibrahim, R.A. Highly Compact 4 × 4 Flower-Shaped MIMO Antenna for Wideband Communications. *Appl. Sci.* **2023**, *13*, 3532. [CrossRef]
38. Wong, K.L.; Jian, M.F.; Li, W.Y. Low-profile wideband four-corner-fed square patch antenna for 5G MIMO mobile antenna application. *IEEE Antennas Wirel. Propag. Lett.* **2021**, *20*, 2554–2558. [CrossRef]
39. Chattha, H.T.; Ishfaq, M.K.; Khawaja, B.A.; Sharif, A.; Sheriff, N. Compact multiport MIMO antenna system for 5G IoT and cellular handheld applications. *IEEE Antennas Wirel. Propag. Lett.* **2021**, *20*, 2136–2140. [CrossRef]
40. Din, I.U.; Kiyani, A.; Naqvi, S.I.; Al-Gburi, A.J.A.; Abbas, S.M.; Ullah, S. A Low-Cost Wideband MIMO Antenna for IoT Applications. In Proceedings of the 2022 IEEE International Symposium on Antennas and Propagation and USNC-URSI Radio Science Meeting (AP-S/URSI), Denver, CO, USA, 10–15 July 2022; pp. 2064–2065. [CrossRef]
41. Jehangir, S.S.; Sharawi, M.S. A compact single-layer four-port orthogonally polarized Yagi-like MIMO antenna system. *IEEE Antennas Wirel. Propag. Lett.* **2020**, *68*, 6372–6377. [CrossRef]
42. Hussain, M.; Mousa Ali, E.; Jarchavi, S.M.R.; Zaidi, A.; Najam, A.I.; Alotaibi, A.A.; Althobaiti, A.; Ghoneim, S.S.M. Design and characterization of compact broadband antenna and its MIMO configuration for 28 GHz 5G applications. *Electronics* **2022**, *11*, 523. [CrossRef]
43. Dayo, Z.A.; Aamir, M.; Dayo, S.A.; Khoso, I.A.; Soothar, P.; Sahito, F.; Zheng, T.; Hu, Z.; Guan, Y. A novel compact broadband and radiation efficient antenna design for medical IoT healthcare system. *Math. Biosci. Eng.* **2022**, *19*, 3909–3927. [CrossRef]
44. Dama, Y.A.S.; Abd-Alhameed, R.A.; Jones, S.M.R.; Zhou, D.; McEwan, N.J.; Child, M.B.; Excell, P.S. An envelope correlation formula for (N, N) MIMO antenna arrays using input scattering parameters, and including power losses. *Int. J. Antennas Propag.* **2011**, *2011*, 421691. [CrossRef]

45. Hussain, N.; Awan, W.A.; Ali, W.; Naqvi, S.I.; Zaidi, A.; Le, T.T. Compact wideband patch antenna and its MIMO configuration for 28 GHz applications. *AEU Int. J. Electron. Commun.* **2021**, *132*, 153612. [CrossRef]
46. Cai, J.; Zhang, J.; Xi, S.; Huang, J.; Liu, G. A Wideband Eight-Element Antenna with High Isolation for 5G New-Radio Applications. *Appl. Sci.* **2023**, *13*, 137. [CrossRef]